Untargeted Metabolomics Combined with Metabolic Flux Analysis Reveals the Mechanism of Sodium Citrate for High S-Adenosyl-Methionine Production by *Pichia pastoris*

Wentao Xu †, Feng Xu †, Weijing Song, Le Dong, Jiangchao Qian and Mingzhi Huang *

State Key Laboratory of Bioreactor Engineering, East China University of Science and Technology, No. 130 Meilong Road, Shanghai 200237, China

* Correspondence: huangmz@ecust.edu.cn

† These authors contributed equally to this work.

Supplementary material

Figure S1. Physiological profiles of *P. pastoris* at the rate of 0.2 g/L/h and 0.4 g/L/h L-methionine supplementation in fed-batch cultivations.

Figure S2. Physiological profiles of *P. pastoris* fermentation under supplementation with sodium citrate.

Figure S3. The multivariate statistical analysis for the samples. Volcano plot of (a) positive ion mode and (b) negative ion mode (color correlates with differential metabolite up- and down-regulation, marked with qualitative names, up- and down-regulation multiplicity); OPLS-DA score in (c) positive ion mode and (d) negative ion mode; Permutation test of OPLS-DA model in (e) positive ion mode and (f) negative ion mode.

Figure S4. The PCA score. (a) Positive ion mode; (b) Negative ion mode.

Table S1. The simplified metabolic network model of *P. pastoris*.

Table S2. The significantly up-regulated differential metabolites.

Table S3. The significantly down-regulated differential metabolites

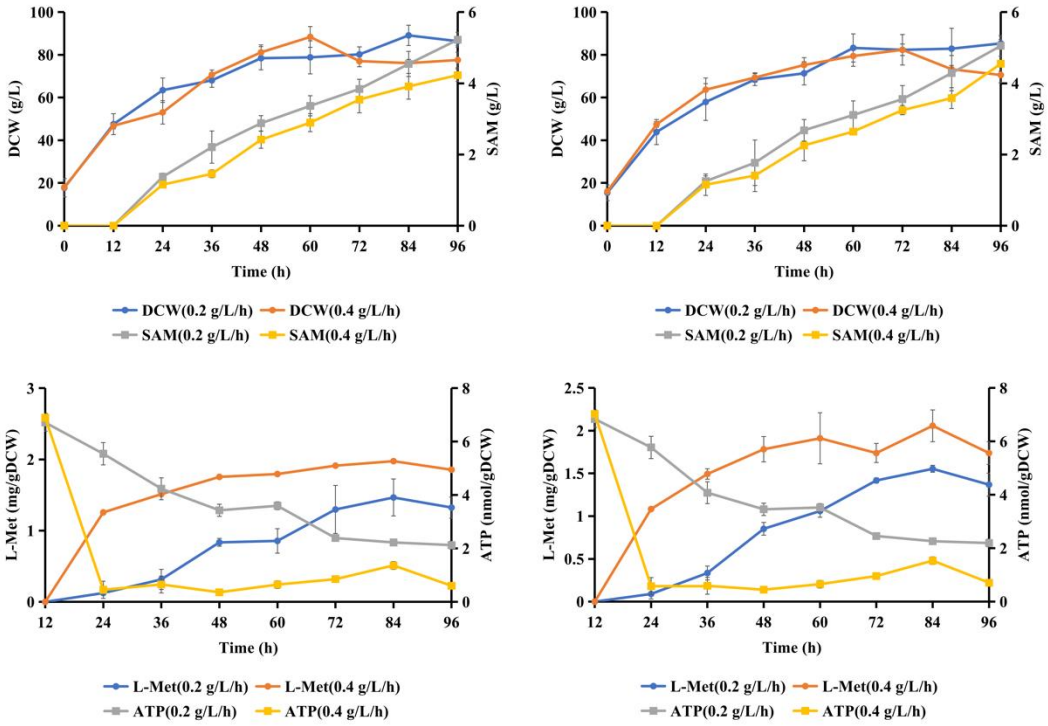

Figure S1. Physiological profiles of *P. pastoris* at the rate of 0.2 g/L/h and 0.4 g/L/h L-methionine supplementation in fed-batch cultivations.

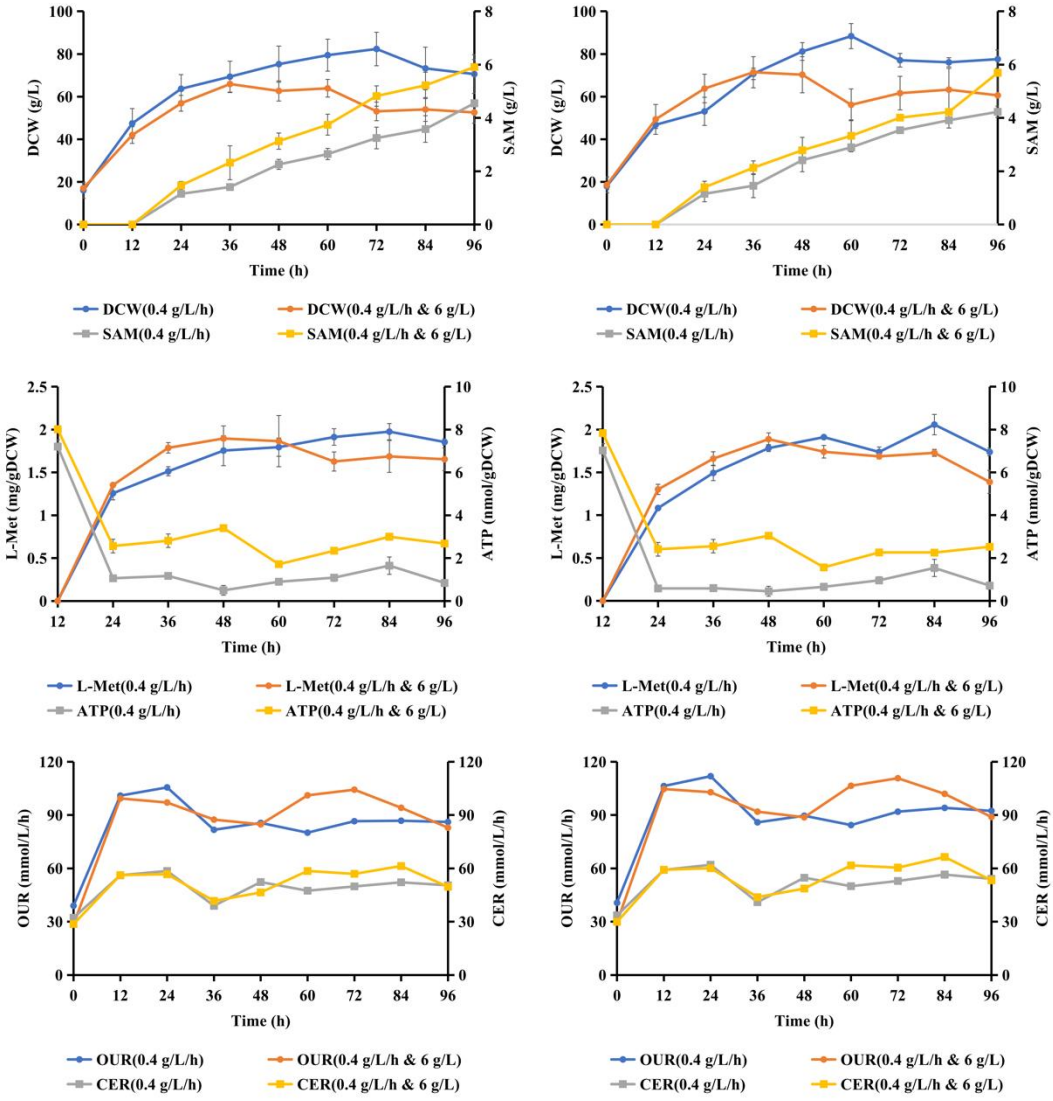

Figure S2. Physiological profiles of *P. pastoris* fermentation under supplementation with sodium citrate.

Sample quality control and statistical analysis

Differential analysis was performed for all metabolites detected in positive and negative ion mode (including unidentified metabolites) based on univariate analysis (Fold Change Analysis, FC Analysis). The differential metabolites were screened with FC > 1.5, and a volcano plot was used to visualize the data (Figure S1a,b). Subsequently, all the metabolites identified previously were reintegrated by principal component analysis (PCA) using a linear combination, and the metabolites in the fermentation broth of the experimental and control groups were compared and analyzed to obtain the PCA models in positive and negative ion mode, respectively. It can be seen from Figure S2 that all samples were within the 95% confidence interval, the aggregation within the group was high, and the differences between the groups were noticeable. Therefore, the biological reproducibility of samples can be considered reliable. The PCA model (R^2X was 0.519) under the positive ion model achieved a model interpretation rate of 51.9%, while the PCA model (R^2X=0.556) under the negative ion model achieved a model interpretation rate of 55.6%. Therefore, the model can be considered stable and used for subsequent analysis.

Given the ability to visually represent the relationship between the class of sample and the expression of interest metabolites, orthogonal partial least squares discrimination analysis (OPLS-DA) is commonly applied to predict the type of samples. The results showed that the data points of both the experimental and control groups were relatively highly aggregated and differed significantly between groups, which was consistent with the results of the PCA model analysis (Figures S1c and S2d). The corresponding score plots for OPLS-DA showed a clear separation between the supplement with and without sodium citrate groups in both positive and negative ion modes, indicating different metabolite compositions between the two groups. In addition, the OPLS-DA model parameters, including $R^2(X)$, $R^2(Y)$, and Q^2, were 0.467, 1.000, and 0.761 in the positive ion mode, respectively, and 0.464, 0.999, and 0.838 in the negative ion model were 0.464, 0.999 and 0.838, respectively. Moreover, the overfitting can be effectively avoided by performing the Permutation test on the OPLS-DA model (Figure S1e,f). Here, the values (R^2 and Q^2) of the stoichiometry model decreased with the gradual fall of the replacement retention. Therefore, the results demonstrated practical reproducibility and predictability in explaining the differences between the two groups.

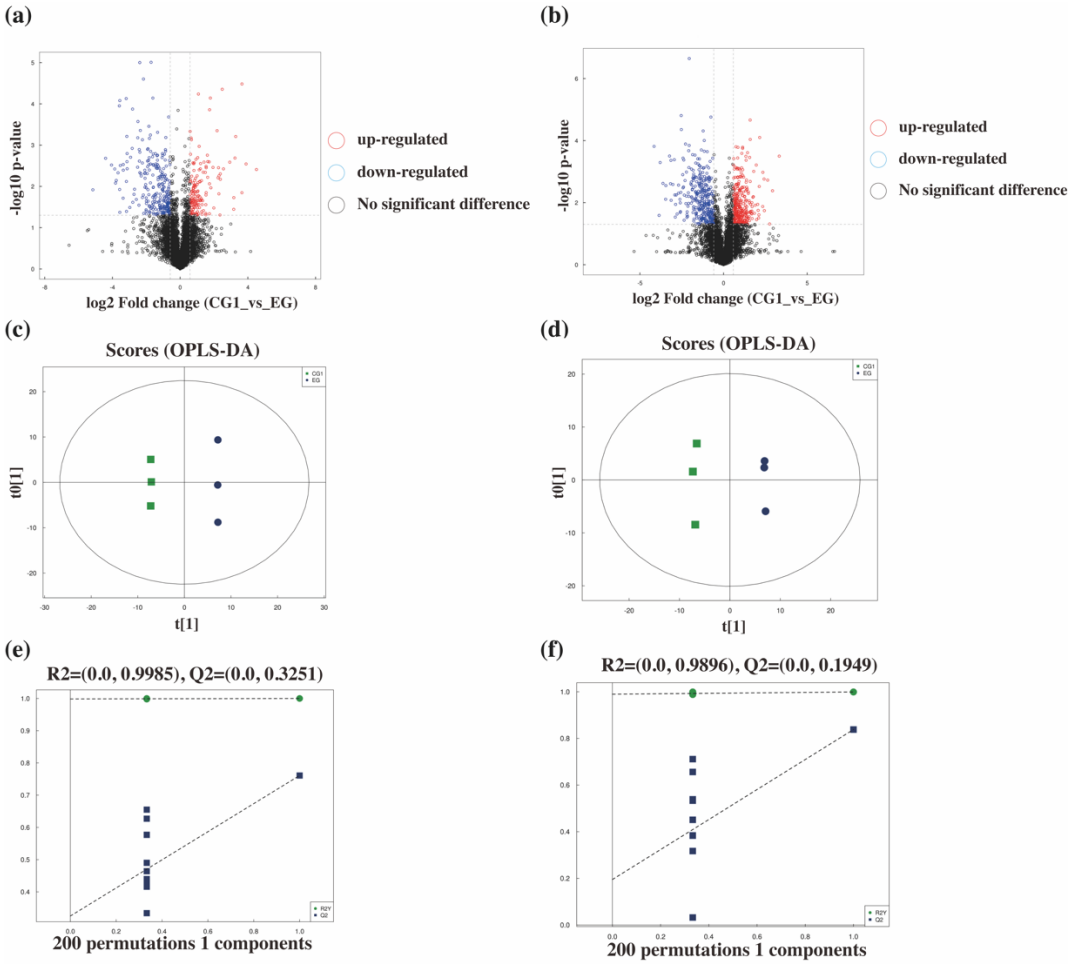

Figure S3. The multivariate statistical analysis for the samples. Volcano plot of (a) positive ion mode and (b) negative ion mode (color correlates with differential metabolite up- and down-regulation, marked with qualitative names, up- and down-regulation multiplicity); OPLS-DA score in (c) positive ion mode and (d) negative ion mode; Permutation test of OPLS-DA model in (e) positive ion mode and (f) negative ion mode.

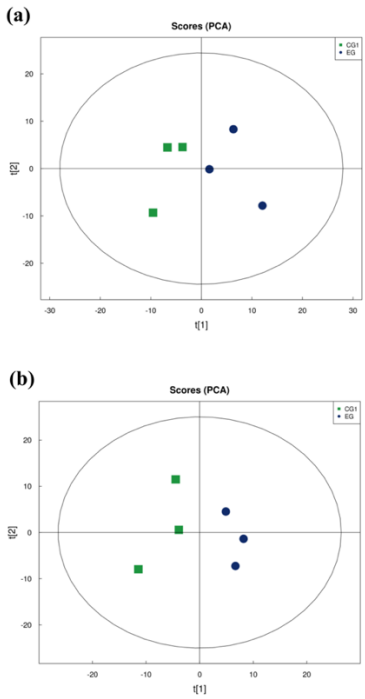

Figure S4. The PCA score. (a) Positive ion mode; (b) Negative ion mode.

Table S1. The simplified metabolic network model of *P. pastoris*.

No.	Reaction
r1	F6P→G6P
r2	2·GAP→F6P + ATP
r3	GAP→Pyr + 2·ATP + NADH
r4	Pyr→AcCoA + NADH + CO2
r5	AcCoA + OAA→Cit
r6	Cit→AKG + NADH + CO2
r7	AKG→SucCoA + NADH + CO2
r8	SucCoA→Suc + ATP
r9	Suc→OAA + NADH + FADH2
r10	Cit + AcCoA→2·OAA + 2·NADH + FADH2
r11	G6P→Ru5P + CO2 + 2·NADPH
r12	Ru5P→Xu5P
r13	Ru5P→R5P
r14	R5P + Xu5P→E4P + F6P
r15	E4P + Xu5P→F6P + GAP
r16	OAA→Pyr + CO2 + ATP
r17	MeOH + O2→H2O2+ PA
r18	PA+ Xu5P + ATP→2·GAP
r19	L-Met→CH3SH + NADH + SucCoA
r20	L-Met + ATP→SAM
r21	NADH + 0.5·O2→2.5·ATP
r22	FADH2 + 0.5·O2→2.5·ATP
r23	OAA→OAA.ex
r24	O2.ex→O2
r25	CO2→CO2.ex
r26	MeOH.ex→MeOH
r27	SAM→SAM.ex
r28	Tri.Ci→Cit
r29	L-Met.ex→L-Met

Table S2. The significantly up-regulated differential metabolites.

#	Metabolites	VIP	FC	P value
1	Cis,cis-muconic acid	6.97	4.20	0.001
2	2-Oxoadipic acid	4.07	3.45	0.0012
3	(-)-quebrachitol	3.59	3.73	0.0012
4	L-saccharopine	2.86	1.35	0.0023
5	3,4-dihydroxyhydrocinnamic acid	1.04	9.01	0.0024
6	Asiatic acid	1.12	1.50	0.0026
7	2-methoxy-5-nitrophenol	1.38	2.70	0.0028
8	alpha.-galactobiose	1.95	1.77	0.0032
9	Xanthydrol	1.56	2.22	0.0049
10	Calycin	1.91	1.93	0.0055
11	Cis-aconitate	4.80	1.89	0.0064
12	Juglone	12.91	1.72	0.0069
13	Tosyl-l-lysyl-chloromethane	1.36	2.36	0.0088
14	4-hydroxyphenylpyruvate	2.11	1.83	0.012
15	Psoralidin	1.15	2.02	0.013
16	Citrate	18.76	2.34	0.015
17	Dihydroxyacetone	6.08	1.98	0.017
18	C17-sphinganine	2.33	1.66	0.022
19	3,5,9-trioxa-4-phosphatetracosan-1-aminium	5.34	1.23	0.023
20	L-Glutamine	1.86	7.41	0.029
21	Apocynin	1.09	1.33	0.031
22	2(1h)-pyridinone	2.19	3.20	0.033
23	Misoprostol	1.80	1.58	0.034
24	2-aminobenzimidazole	1.54	2.49	0.036
25	1-hydroxy vitamin d2	2.42	1.55	0.040

Table S3. The significantly down-regulated differential metabolites.

#	Metabolites	VIP	FC	P value
1	Glutathione	7.42	0.60	0.0002
2	Lpc 18:1	15.37	0.82	0.0011
3	Carnitine	7.22	0.49	0.0020
4	4-oxobutanoic acid	3.20	0.82	0.0025
5	Lpc 18:2	9.61	0.88	0.0044
6	Dibutyl phthalate	1.09	0.79	0.0064
7	1-Palmitoyl-sn-glycero-3-phosphocholine	5.79	0.80	0.0091
8	Benzoic acid	3.41	0.89	0.017
9	Prednisone	1.67	0.32	0.019
10	1-oleoyl-sn-glycero-3-phosphoethanolamine	4.10	0.66	0.023
11	Phe-Phe-Arg	1.72	0.73	0.024
12	5-aminosalicylic acid	1.61	0.66	0.024
13	Glycerophosphocholine	13.72	0.94	0.027
14	Asparagine	3.41	0.63	0.037
15	Diarylheptanoids	1.28	0.79	0.039
16	Adenine	8.30	0.61	0.045